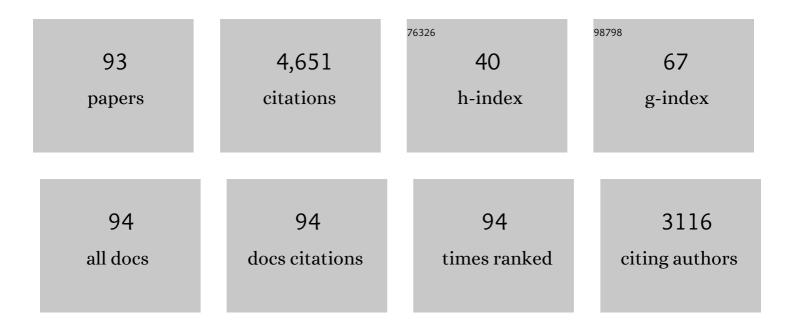
List of Publications by Year in descending order

Source: https://exaly.com/author-pdf/3629627/publications.pdf Version: 2024-02-01



Γινοπικά Λοάγοιο

#	Article	IF	CITATIONS
1	Phonon Density of States of Iron up to 153 Gigapascals. Science, 2001, 292, 914-916.	12.6	284
2	The viscosity of liquid iron at the physical conditions of the Earth's core. Nature, 1998, 392, 805-807.	27.8	259
3	Possible thermal and chemical stabilization of body-centred-cubic iron in the Earth's core. Nature, 2003, 424, 536-539.	27.8	249
4	Thermal expansion and crystal structure of cementite, Fe3C, between 4 and 600â€K determined by time-of-flight neutron powder diffraction. Journal of Applied Crystallography, 2004, 37, 82-90.	4.5	186
5	Ammonium sulfate on Titan: Possible origin and role in cryovolcanism. Icarus, 2007, 188, 139-153.	2.5	157
6	First-principles modelling of Earth and planetary materials at high pressures and temperatures. Reports on Progress in Physics, 2006, 69, 2365-2441.	20.1	152
7	The properties of iron under core conditions from first principles calculations. Physics of the Earth and Planetary Interiors, 2003, 140, 101-125.	1.9	138
8	Ab initiomelting curve of the fcc phase of aluminum. Physical Review B, 2002, 65, .	3.2	124
9	Ab initio calculations of the elasticity of iron and iron alloys at inner core conditions: Evidence for a partially molten inner core?. Earth and Planetary Science Letters, 2007, 254, 227-232.	4.4	119
10	Thermal expansion and crystal structure of FeSi between 4 and 1173 K determined by time-of-flight neutron powder diffraction. Physics and Chemistry of Minerals, 2002, 29, 132-139.	0.8	113
11	The effect of ferromagnetism on the equation of state of Fe 3 C studied by first-principles calculations. Earth and Planetary Science Letters, 2002, 203, 567-575.	4.4	108
12	Crystal structure, compressibility and possible phase transitions in oldvarepsilon-FeSi studied by first-principles pseudopotential calculations. Acta Crystallographica Section B: Structural Science, 1999, 55, 484-493.	1.8	107
13	First principles calculations on crystalline and liquid iron at Earth's core conditions. Faraday Discussions, 1997, 106, 205-218.	3.2	106
14	In situ measurement of viscosity of liquids in the Fe-FeS system at high pressures and temperatures. American Mineralogist, 2000, 85, 1838-1842.	1.9	101
15	Ab initio calculations of the elasticity of hcp-Fe as a function of temperature at inner-core pressure. Earth and Planetary Science Letters, 2009, 288, 534-538.	4.4	97
16	Strong Premelting Effect in the Elastic Properties of hcp-Fe Under Inner-Core Conditions. Science, 2013, 342, 466-468.	12.6	95
17	Ab initio free energy calculations on the polymorphs of iron at core conditions. Physics of the Earth and Planetary Interiors, 2000, 117, 123-137.	1.9	89
18	A new high-pressure phase of FeSi. American Mineralogist, 2002, 87, 784-787.	1.9	72

#	Article	IF	CITATIONS
19	Grüneisen parameters and isothermal equations of state. American Mineralogist, 2000, 85, 390-395.	1.9	70
20	The long-term stability of a possible aqueous ammonium sulfate ocean inside Titan. Icarus, 2008, 197, 137-151.	2.5	69
21	Light elements in the Earth's core. Nature Reviews Earth & Environment, 2021, 2, 645-658.	29.7	69
22	Ab initiomelting curve of copper by the phase coexistence approach. Journal of Chemical Physics, 2004, 120, 2872-2878.	3.0	68
23	The melting of MgO — computer calculations via molecular dynamics. Physics and Chemistry of Minerals, 1996, 23, 42-49.	0.8	64
24	The effect of nickel on the properties of iron at the conditions of Earth's inner core: Ab initio calculations of seismic wave velocities of Fe–Ni alloys. Earth and Planetary Science Letters, 2013, 365, 143-151.	4.4	62
25	The equation of state of CsCl-structured FeSi to 40 GPa: Implications for silicon in the Earth's core. Geophysical Research Letters, 2003, 30, 14-1-14-4.	4.0	59
26	Melting curve of materials: theory versus experiments. Journal of Physics Condensed Matter, 2004, 16, S973-S982.	1.8	59
27	The elastic properties of hcp-Fe alloys under the conditions of the Earth's inner core. Earth and Planetary Science Letters, 2018, 493, 118-127.	4.4	59
28	First principles calculations on the diffusivity and viscosity of liquid Fe–S at experimentally accessible conditions. Physics of the Earth and Planetary Interiors, 2000, 120, 145-152.	1.9	58
29	The high-pressure phase diagram of ammonia dihydrate. High Pressure Research, 2007, 27, 201-212.	1.2	57
30	The Earth's core as a reservoir of water. Nature Geoscience, 2020, 13, 453-458.	12.9	56
31	The melting curve of Ni to 1 Mbar. Earth and Planetary Science Letters, 2014, 408, 226-236.	4.4	55
32	The thermoelastic properties of MgSO47D2O (epsomite) from powder neutron diffraction and ab initio calculation. European Journal of Mineralogy, 2006, 18, 449-462.	1.3	50
33	High-pressure phase transformations of FeS: Novel phases at conditions of planetary cores. Earth and Planetary Science Letters, 2008, 272, 481-487.	4.4	50
34	The structure of iron under the conditions of the Earth's inner core. Geophysical Research Letters, 1999, 26, 1231-1234.	4.0	47
35	Hydrogen bonding in solid ammonia fromab initiocalculations. Journal of Chemical Physics, 2003, 118, 5987-5994.	3.0	47
36	The incompressibility and thermal expansivity of D2O ice II determined by powder neutron diffraction. Journal of Applied Crystallography, 2005, 38, 612-618.	4.5	47

#	Article	IF	CITATIONS
37	Absolute ionic diffusion in MgO—computer calculations via lattice dynamics. Physics of the Earth and Planetary Interiors, 1995, 88, 193-210.	1.9	44
38	Ab initio simulation of ammonia monohydrate (NH3â‹H2O) and ammonium hydroxide (NH4OH). Journal of Chemical Physics, 2001, 115, 7006-7014.	3.0	44
39	Melting properties from <i>ab initio</i> free energy calculations: Iron at the Earth's inner-core boundary. Physical Review B, 2018, 98, .	3.2	43
40	The thermal expansion and crystal structure of mirabilite (Na2SO4·10D2O) from 4.2 to 300ÂK, determined by time-of-flight neutron powder diffraction. Physics and Chemistry of Minerals, 2009, 36, 29-46.	0.8	42
41	The thermal expansion of gold: point defect concentrations and pre-melting in a face-centred cubic metal. Journal of Applied Crystallography, 2018, 51, 470-480.	4.5	41
42	Melting curve of copper measured to 16ÂGPa using a multi-anvil press. High Pressure Research, 2006, 26, 185-191.	1.2	39
43	Light elements in the core: Effects of impurities on the phase diagram of iron. Geophysical Research Letters, 2008, 35, .	4.0	38
44	A high-resolution neutron powder diffraction study of ammonia dihydrate (ND3â‹2D2O) phase I. Journal of Chemical Physics, 2003, 119, 10806-10813.	3.0	37
45	The NiSi melting curve to 70GPa. Physics of the Earth and Planetary Interiors, 2014, 233, 13-23.	1.9	36
46	Crystal structures and thermal expansion of α-MgSO4and β-MgSO4from 4.2 to 300â€K by neutron powder diffraction. Journal of Applied Crystallography, 2007, 40, 761-770.	4.5	35
47	The stability of bcc-Fe at high pressures and temperatures with respect to tetragonal strain. Physics of the Earth and Planetary Interiors, 2008, 170, 52-59.	1.9	34
48	Phase behaviour and thermoelastic properties of perdeuterated ammonia hydrate and ice polymorphs from 0 to 2â€GPa. Journal of Applied Crystallography, 2009, 42, 846-866.	4.5	32
49	Ab initio calculations on the free energy and high P–T elasticity of face-centred-cubic iron. Earth and Planetary Science Letters, 2008, 268, 444-449.	4.4	31
50	The structure, ordering and equation of state of ammonia dihydrate (nh3 · 2h2o). Icarus, 2003, 162, 59-73.	2.5	30
51	Strong shear softening induced by superionic hydrogen in Earth's inner core. Earth and Planetary Science Letters, 2021, 568, 117014.	4.4	29
52	Ab initio simulation of the ice II structure. Journal of Chemical Physics, 2003, 119, 4567-4572.	3.0	28
53	Thermoelasticity of Fe <sub>7</sub> C <sub>3</sub> under inner core conditions. Journal of Geophysical Research: Solid Earth, 2016, 121, 5828-5837.	3.4	28
54	The effect of silicon impurities on the phase diagram of iron and possible implications for the Earth's core structure. Journal of Physics and Chemistry of Solids, 2008, 69, 2177-2181.	4.0	26

#	Article	IF	CITATIONS
55	The elastic properties of hcp-Fe 1â^'x Si x at Earth's inner-core conditions. Earth and Planetary Science Letters, 2016, 451, 89-96.	4.4	25
56	Carbon Partitioning Between the Earth's Inner and Outer Core. Journal of Geophysical Research: Solid Earth, 2019, 124, 12812-12824.	3.4	23
57	Experimental verification of the Stokes-Einstein relation in liquid Fe—FeS at 5 GPa. Molecular Physics, 2001, 99, 773-777.	1.7	21
58	An ab initio study of the relative stabilities and equations of state of FeS polymorphs. Mineralogical Magazine, 2001, 65, 181-191.	1.4	21
59	Ab initio lattice dynamics calculations on the combined effect of temperature and silicon on the stability of different iron phases in the Earth's inner core. Physics of the Earth and Planetary Interiors, 2010, 178, 2-7.	1.9	20
60	An ab initio study of nickel substitution into iron. Earth and Planetary Science Letters, 2006, 248, 147-152.	4.4	18
61	Equation of state and pressure-induced structural changes in mirabilite (Na2SO4·10H2O) determined from ab initio density functional theory calculations. Physics and Chemistry of Minerals, 2010, 37, 265-282.	0.8	17
62	Structures and physical properties of â^Š-FeSi-type and CsCl-type RuSi studied by first-principles pseudopotential calculations. Acta Crystallographica Section B: Structural Science, 2000, 56, 369-376.	1.8	16
63	High pressure stability of the monosilicides of cobalt and the platinum group elements. Journal of Alloys and Compounds, 2015, 626, 375-380.	5.5	16
64	The elastic properties and stability of fcc-Fe and fcc-FeNi alloys at inner-core conditions. Geophysical Journal International, 2015, 202, 94-101.	2.4	16
65	Thermoelastic properties of magnesiowüstite, (Mg <sub>1â^'<i>x</i></sub> Fe <sub><i>x</i></sub> )O: determination of the Anderson–Grüneisen parameter by time-of-flight neutron powder diffraction at simultaneous high pressures and temperatures. Journal of Applied Crystallography, 2008, 41, 886-896.	4.5	15
66	The phase diagrams of KCaF3 and NaMgF3 by ab initio simulations. Physics and Chemistry of Minerals, 2018, 45, 311-322.	0.8	15
67	First principles calculations on the high-pressure behavior of magnesite. American Mineralogist, 1999, 84, 1627-1631.	1.9	14
68	<i>P</i> – <i>V</i> – <i>T</i> equation of state of synthetic mirabilite (Na <sub>2</sub> SO <sub>4</sub> ·10D <sub>2</sub> O) determined by powder neutron diffraction. Journal of Applied Crystallography, 2013, 46, 448-460.	4.5	14
69	High-pressure phase transitions and equations of state in NiSi. I. <i>Ab initio</i> simulations. Journal of Applied Crystallography, 2012, 45, 186-196.	4.5	13
70	The isothermal equation of state of CaPtO3 post-perovskite to 40GPa. Physics of the Earth and Planetary Interiors, 2010, 182, 113-118.	1.9	12
71	High-pressure phase transitions and equations of state in NiSi. III. A new high-pressure phase of NiSi. Journal of Applied Crystallography, 2013, 46, 14-24.	4.5	12
72	The top-down crystallisation of Mercury's core. Earth and Planetary Science Letters, 2019, 528, 115838.	4.4	11

#	Article	IF	CITATIONS
73	Thermoelastic properties and crystal structure of CaPtO <sub>3</sub> post-perovskite from 0 to 9â€GPa and from 2Âto 973â€K. Journal of Applied Crystallography, 2011, 44, 999-1016.	4.5	10
74	High-pressure phase transitions and equations of state in NiSi. II. Experimental results. Journal of Applied Crystallography, 2012, 45, 726-737.	4.5	10
75	Equation of State of hcp Feâ€Câ€Si Alloys and the Effect of C Incorporation Mechanism on the Density of hcp Fe Alloys at 300ÂK. Journal of Geophysical Research: Solid Earth, 2020, 125, e2020JB020159.	3.4	10
76	Atomic transport properties of liquid iron at conditions of planetary cores. Journal of Chemical Physics, 2021, 155, 194505.	3.0	9
77	The phase diagram of NiSi under the conditions of small planetary interiors. Physics of the Earth and Planetary Interiors, 2016, 261, 196-206.	1.9	8
78	Mg partitioning between solid and liquid iron under the Earth's core conditions. Physics of the Earth and Planetary Interiors, 2018, 274, 218-221.	1.9	8
79	High-temperature ab initio calculations on FeSi and NiSi at conditions relevant to small planetary cores. Physics and Chemistry of Minerals, 2017, 44, 477-484.	0.8	7
80	Anisotropic diffusion creep in postperovskite provides a new model for deformation at the coreâ°mantle boundary. Proceedings of the National Academy of Sciences of the United States of America, 2019, 116, 26389-26393.	7.1	7
81	Molecular dynamics: some recent developments in classical and quantum mechanical simulation of minerals. Mineralogical Magazine, 1995, 59, 597-605.	1.4	7
82	The Earth's deep interior: advances in theory and experiment. Philosophical Transactions Series A, Mathematical, Physical, and Engineering Sciences, 1999, 357, 3335-3357.	3.4	6
83	An ab initio study of the relative stabilities and equations of state of Fe3S polymorphs. Mineralogical Magazine, 2004, 68, 813-817.	1.4	6
84	Primitive noble gases sampled from ocean island basalts cannot be from the Earth's core. Nature Communications, 2022, 13, .	12.8	6
85	The thermal expansion of (Fe <sub>1â^'<i>y</i></sub> Ni <sub><i>y</i></sub> )Si. Journal of Physics Condensed Matter, 2017, 29, 335701.	1.8	5
86	ElasT: A toolkit for thermoelastic calculations. Computer Physics Communications, 2022, 273, 108280.	7.5	3
87	Thermal Properties of Liquid Iron at Conditions of Planetary Cores. Journal of Geophysical Research E: Planets, 0, , .	3.6	3
88	The effect of water on the outer core transport properties. Physics of the Earth and Planetary Interiors, 2022, 329-330, 106907.	1.9	3
89	The equation of state of thePmmnphase of NiSi. Journal of Applied Crystallography, 2015, 48, 1914-1920.	4.5	2
90	New Views of the Earth's Inner Core from Computational Mineral Physics. , 2009, , 397-412.		1

#	Article	IF	CITATIONS
91	Core composition revealed. Nature, 2013, 495, 177-178.	27.8	1
92	The Theory and Simulation of the Melting of Minerals. , 1999, , 561-575.		1
93	Equation of state for CO and CO2 fluids and their application on decarbonation reactions at high pressure and temperature. Chemical Geology, 2021, 559, 119918.	3.3	0